Soft Matter

COMMUNICATION

Switching of carbohydrate nanofibers for regulating cell proliferation†

Guangren Na, Ying He, Yongju Kim and Myongsoo Lee*

Cite this: *Soft Matter*, 2016, **12**, 2846

Received 20th December 2015,
Accepted 18th February 2016

DOI: 10.1039/c5sm03073k

www.rsc.org/softmatter

We report switchable, fluorescent carbohydrate nanofibers formed through the self-assembly of aromatic rod amphiphiles with a combination of mannose epitopes and thermoresponsive oligoether dendrons. The carbohydrate nanofibers undergo reversible switching between carbohydrate-exposed and hidden states on their surface in response to a thermal signal, and have the ability to regulate cell proliferation.

Carbohydrates present on the surfaces of cells mediate many biological processes such as cell growth regulation, immune response, and inflammation by viruses and bacteria that are fundamentally important for both healthy and diseased states of the living organism.[1] To regulate or suppress a wide range of the biological processes, multivalent carbohydrate ligands are required because monovalent ligands are poorly recognized by carbohydrate-binding proteins.[2] Multivalent ligands can bind to receptor proteins with high avidity and specificity, thereby serving as powerful inhibitors because they present multiple copies of a receptor-binding epitope with high cooperativity for binding events.[3–5] The simultaneous presentation of carbohydrate epitopes on an appropriate macromolecular scaffold creates a multivalent display that amplifies the affinity of carbohydrate-mediated receptor targeting. Typical examples include oligosaccharides, glycopolymers, and glycodendrimers that exhibit multiple and cooperative receptor binding properties.[6] Despite these advances in multivalent carbohydrate ligands, the incorporation of both sensing and switching characteristics into multivalent systems to externally control physiological processes is limited.[7] This is most probably because they are mostly too inflexible to undergo dynamic switching between active and inactive states without structural collapse.

Non-covalent supramolecular assemblies of amphiphilic carbohydrate modules provide a facile means to allow addressing these limitations by forming dynamic multivalent scaffolds.[8–10] A large number of amphiphilic modules have been developed that self-assemble into supramolecular nanostructures such as vesicles, micelles, and nanofibers of different sizes and functionalities.

For example, peptide amphiphiles containing carbohydrate units form well-defined carbohydrate nanoribbons that agglutinate specific bacterial cells.[11,12] Supramolecular columns formed through the self-assembly of discotic carbohydrate modules also bind lectins at bacterial cell surfaces.[13] Rod-coil molecular architectures provide another example of supramolecular scaffolds for multivalent carbohydrate nanostructures. We have shown that carbohydrate nanostructures can be readily controlled by small changes in the rod-coil molecular architecture, which regulate the biological activities of bacterial cells.[14,15] In addition, we have also shown that the crystallinity of the rod building blocks plays a crucial role in controlling the length of the carbohydrate-coated nanofibers.[16] Furthermore, the binding properties of the carbohydrate-coated nanofibers revealed that the length of the fibers has a significant influence both on the formation of bacterial clusters and on the regulation of the proliferation of bacterial cells.

However, most of the self-assembled carbohydrate nanofibers are far from dynamic switching between binding and non-binding states with bacterial cells to mimic the sophisticated dynamics of biological interactions and thus, to precisely regulate biological activities.[12,17] Therefore, the challenging target in artificial self-assembly is to confer both switching and sensing functions with carbohydrate nanofibers without compromising their intrinsic features. To address this challenge, we considered that the coassembly of a carbohydrate amphiphile with an amphiphilic rod molecule based on a laterally grafted oligoether dendron could endow fluorescent carbohydrate nanofibers with switching functions triggered by controlled dehydration of oligoether chains.[18]

Here, we report fluorescent carbohydrate nanofibers that undergo reversible switching between carbohydrate-exposed and hidden states for the capture and release of specific bacterial cells triggered by a thermal signal. The thermal switching of the

State Key Lab of Supramolecular Structure and Materials, College of Chemistry, Jilin University, Changchun 130012, China. E-mail: mslee@jlu.edu.cn

† Electronic supplementary information (ESI) available: Experimental details, FOM images, TEM images, and spectroscopic data. See DOI: 10.1039/c5sm03073k

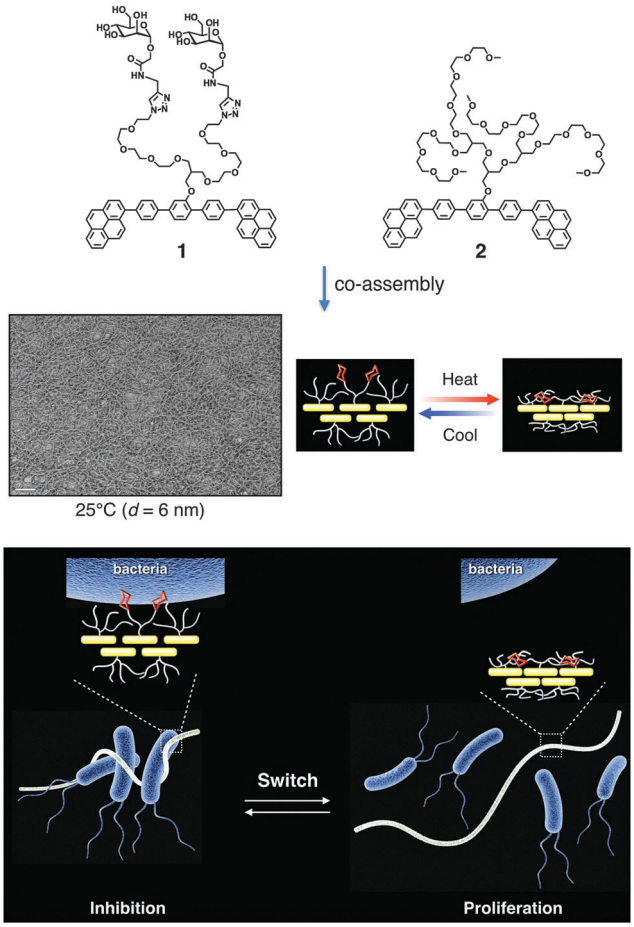

Fig. 1 The chemical structure of amphiphiles **1** and **2**, TEM images of co-assembled nanofibers in aqueous solution at different temperatures (scale bar, 100 nm). Schematic representation of switching of carbohydrate nanofibers in binding and releasing bacteria.

nanofibers subsequently regulates the proliferation of bacterial cells through controlled multivalent carbohydrate–protein interactions (Fig. 1). The fluorescent carbohydrate nanofibers with a switching function are comprised of rod amphiphile **1** based on carbohydrate units and rod amphiphile **2** based on an oligoether dendron. The self-assembling molecules were synthesized in a stepwise manner according to the procedures described previously.[16,19] Transmission electron microscopy (TEM) revealed that both **1** and **2** self-assemble into micrometer-long nanofibers with an average diameter of 6 nm (Fig. S1, ESI†). We considered that an increasing content of **2** in the coassembled nanofibers would lead to the decrease of the carbohydrate density on the nanofiber surfaces, while rendering the nanofibers with stimulus-responsiveness due to thermal dehydration of the oligoether dendron. Accordingly, we performed coassembly experiments with different mole ratios of **1** and **2**. Similar to the dimensions of each pure nanofiber of **1** and **2**, indeed, all of the coassembled nanofibers were seen to be micrometer-long in length and ~6 nm in diameter, indicating that the coassembly of **1** with **2** does not influence on the nanostructure in length together with a lateral dimension (Fig. 1). All of the assembled nanofibers displayed similar absorption and emission characteristics, that is, the absorption maximum at ~357 nm and emission at ~446 nm (Fig. S2, ESI†), indicating that the carbohydrate nanofibers are suitable for fluorescence sensing applications to detect specific bacterial cells.[5]

An important feature of the coassembled nanofibers generated *via* the self-assembly of carbohydrate functionalized building blocks with non-carbohydrate dendrons should be the facile and reproducible control over ligand density. The binding epitope density of a multivalent ligand plays a key role in its binding activity to protein receptors.[20] To investigate the effect of carbohydrate density on cell clustering, mannose nanofibers containing different amounts of the oligoether dendron amphiphile **2** were subsequently prepared to decrease the mannose density on the nanofiber surface, ranging from 10 mol% to 90 mol% of **2**. To determine the influence of the mannose density on protein binding, we selected an *E. coli* strain expressing the mannose-binding adhesion protein *Fim H* in its type-1 pili (ORN-178). When the *E. coli* were incubated with the coassembled nanofibers containing up to 50 mol% of **2**, the formation of fluorescent bacterial clusters was observed (Fig. 2a), indicating that the coassembled nanofibers bind to the bacterial cells through multivalent interactions even at 50 mol% of **2**. Above 70 mol% of **2**, however, the coassembled nanofibers did not show bacterial cluster formation, indicating that the critical mannose density of the coassembled nanofibers required for binding activity with the bacterial cell is 50 mol% of **2**. This is further confirmed by TEM investigations of the ORN-178 strain incubated with the co-assembled nanofiber solution at 25 °C (Fig. 2b and 3c). The image showed that the nanofibers bound to type 1 pili in winding of the pili interconnecting one another,

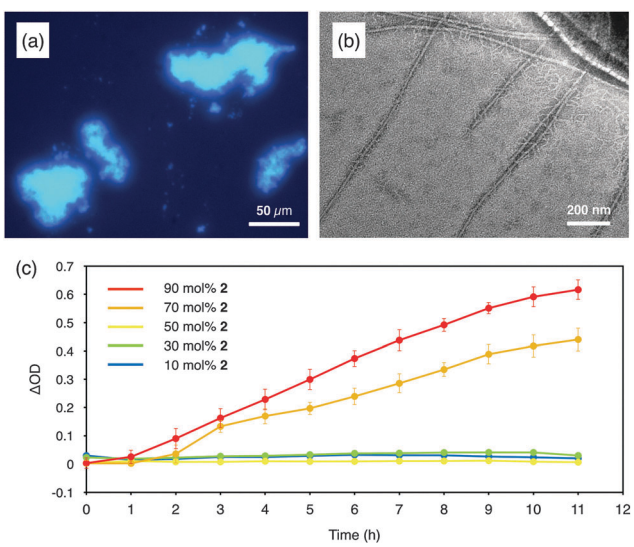

Fig. 2 (a) A representative microscopy image from fluorescence colocalization studies of *E. coli* with nanofibers (30 mol% of **2**) under excitation filter at λ_{ex} = 340–480 nm, indicative of fluorescence of nanofibers. (b) A representative TEM image of *E. coli* with co-assembled nanofibers of 0.02 wt% aqueous solution from 30 mol% of **2**. (c) Growth curves based on the optical density (OD) at 600 nm for *E. coli* grown in the presence of coassembled amphiphiles for 11 h. Each value represents the mean ± SD of three independent experiments.

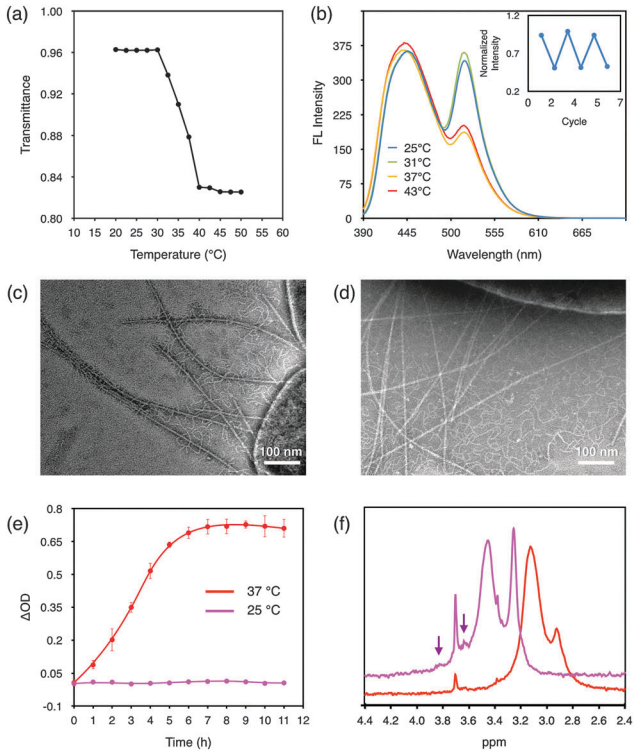

Fig. 3 (a) Transmittance measurement for co-assembly of 50 mol% of **2** in aqueous solution (0.02 wt%) at 500 nm wavelength. (b) Fluorescence spectra of 50 mol% of **2** in coassembled aqueous solution (0.02 wt%) with ConA at different temperatures (excited at 357 nm). Inset is reversible switching cycles of the intensity at 520 nm. TEM images of the pili with coassembled nanofibers (50 mol% of **2**) at (c) 25 °C and (d) 37 °C. (e) Growth curves based on the optical density (OD) at 600 nm for *E. coli* grown in the presence of coassembled amphiphiles (50 mol% of **2**) for 11 h at 25 °C (magenta line) and 37 °C (red line). Each value represents the mean ± SD of three independent experiments. (f) ^{1}H-NMR spectra of coassembled amphiphiles with 50 mol% of **2** in D_2O at 25 °C (magenta line) and 45 °C (red line). The arrows point to the positions of ~3.62 and ~3.83 ppm.

which accounts for the formation of bacteria clusters. We were not able to observe any noticeable disagglutination even after several days of incubation, demonstrating the high stability of the nanofibers in the bacterial clusters.

As reported previously,[21,22] there is a close relationship between the formation of bacterial clusters and the repression of the proliferation activity of bacteria cells. This result stimulated us to envision that the carbohydrate density would affect the size of the bacterial clusters and, subsequently, control bacterial proliferation. To prove this hypothesis, we examined *E. coli* proliferation with the coassembled nanofibers of different carbohydrate densities. Spectrophotometric analysis based on turbidity or optical density (OD) is widely used to estimate the number of bacteria in liquid cultures.[23,24] As the population of bacterial cells grows, the intensity of transmitted light decreases. As the first step in proliferation experiments, an overnight culture of the *E. coli* strain ORN-178 in Luria–Bertani (LB) medium was diluted in phosphate-buffered saline (PBS) until the OD at 600 nm (OD_{600}) was 1.1–1.2. The *E. coli* suspension was mixed with aliquots of the coassembled nanofiber samples in PBS. We measured the variation in the size of the *E. coli* population by measuring OD_{600} every one hour. As shown in Fig. 2c, normal bacterial growth curves were observed in the coassembled nanofibers containing 90 mol% and 70 mol% of **2**, respectively, in which the slope increases with the increasing **2** content. In contrast, we did not observe any noticeable increase in the cell population for the coassembled nanofibers containing less than 50 mol% of **2** during our experimental time range. This result indicates that the proliferation of bacterial cells is inhibited even though the nanofiber includes 50 mol% of **2** based on a non-carbohydrate, oligoether dendron.

The observed results suggest that the coassembled nanofibers may exhibit proliferation switching characteristics because the thermally regulated dehydration of the ethylene oxide chains would hide the carbohydrate epitopes inside the collapsed nanofiber surface.[18,19b] To confirm the switchable properties of the mannose nanofibers triggered by a thermal signal, we selected the coassembled nanofiber containing 50 mol% of **2**. Indeed, the temperature-dependent transmittance of the aqueous solutions of the coassembled nanofibers showed a sharp phase transition at about 35 °C (Fig. 3a), indicating that the ethylene oxide chains with open conformations are dehydrated to collapse upon heating. TEM showed that the nanofiber structures remained unchanged with an individually dispersed state even above 35 °C, demonstrating that the coassembled nanofibers are stable without further aggregation even after dehydration of the oligoether chains (Fig. S3, ESI†). However, the nanofiber size decreases from 6 nm to 5 nm in diameter, indicating that the oligoether chains on the fiber surface are shrunk due to dehydration.[19b,25] The result implies that the mannose epitopes are buried between the dehydrated oligoether dendrons on the nanofiber surfaces above the transition temperature, which will be discussed later.

To corroborate the reversible display of the mannose epitopes on the nanofiber surface triggered by a thermal signal, we performed fluorescence resonance energy transfer (FRET) experiments using fluorescein-labeled Concanavalin A (ConA). The binding of ConA to the mannose on the nanofiber surface is expected to bring the nanofibers and ConA in close proximity and enable energy transfer from the aromatic segment donor to the acceptor fluorescein.[26] Indeed, the addition of ConA resulted in a decrease in the emission of the amphiphilic molecules at 446 nm and the appearance of an acceptor emission peak at 520 nm (Fig. 3b). This result indicates that the carbohydrate ligands effectively bind ConA through specific ligand–protein interactions at room temperature. In great contrast, when the solution was heated to 37 °C, the emission peak associated with FRET is dramatically reduced, indicating that the coassembled nanofibers above the transition lose their binding activity. The experiment could be repeated for subsequent heating–cooling cycles with consistent oscillation in the fluorescence intensity (Fig. 3b, inset), thus demonstrating the reversible binding in a switchable manner. The lost binding activity of the nanofiber upon heating is attributed to a considerable decrease in the concentration of the mannose epitopes exposed on the nanofiber surface.

Considering that the mannose epitopes of the coassembled nanofibers could be reversibly hidden and revealed by a thermal

switch, we envisioned that the nanofibers would reversibly agglutinate bacterial cells upon heating–cooling cycles and, subsequently, control bacterial proliferation. With this idea in mind, we carried out bacterial binding assays with the coassembled nanofiber containing 50 mol% of **2** and a fluorescent protein-labeled *E. coli* strain (ORN-178). When the *E. coli* were incubated with the coassembled nanofiber at room temperature, the large clusters of the fluorescent bacterial cells were observed. Upon heating to 37 °C, however, the cell clusters disappear, demonstrating that the binding activity of the coassembled nanofibers to the bacterial cells is lost upon heating (Fig. S4 and S5, ESI†). This result is consistent with that obtained from the FRET experiments with ConA. To further corroborate the reversible binding of the nanofibers, we performed TEM experiments with the coassembled nanofiber solution (50 mol% of **2**) upon heating (Fig. 3d). At room temperature, the image shows that the nanofibers are wound around the pili, indicative of the strong binding of the coassembled nanofibers to the mannose binding proteins on the pili. In great contrast, upon heating to 37 °C, the nanofibers are seen to be detached from the pili, again demonstrating that the binding activity of the nanofibers is lost upon heating. We next measured the optical density (OD) to examine the *E. coli* proliferation in the presence of the coassembled nanofiber with 50% of **2** (Fig. 3e). At room temperature, spectroscopic measurements do not lead to any changes in the OD value over a period of 11 h, indicating that the nanofiber inhibits efficiently the cell proliferation during our experimental time range. Remarkably, the solution at 37 °C showed a normal bacterial growth curve, demonstrating that the nanofiber does not inhibit the proliferation of bacterial cells.

These results could be understood by considering the reversible display of the mannose epitopes on the nanofiber surfaces in response to a thermal signal. Upon heating, the hydrophobic collapse of the oligoether dendrons on the nanofiber surfaces would enforce the mannose epitopes to be hidden from the nanofiber surfaces.[25] As a consequence, the multivalent interactions between the nanofibers and the bacterial cells are sufficiently weak to facilitate cell proliferation. Upon cooling, however, the rehydration of the oligoether dendrons leads the mannose epitopes to be exposed toward the protein receptors, recovering the strong enough multivalent interactions to promote bacterial aggregation that inhibits cell proliferation. To gain insight into the reversible exposure of the mannose epitopes, we performed temperature-dependent ^{1}H-NMR experiments with the coassembled nanofibers (50 mol% of **2**, D_2O). The spectrum showed broad proton signals at the chemical shift range of 3.1–3.9 ppm associated with the combination of mannose and oligoether backbones (Fig. 3f and Fig. S6, ESI†). Upon heating, the broad signals are upfield-shifted due to the dehydration of the oligoether dendrons and the characteristic mannose signals at ~3.62 and ~3.83 ppm, respectively, nearly disappear,[27,28] indicating that the mannose epitopes are mostly surrounded by the dehydrated oligoether dendrons without exposure from the nanofiber surfaces.

In conclusion, we have demonstrated that a combination of the aromatic amphiphiles based on an oligoether dendron and carbohydrate epitopes generates fluorescent carbohydrate nanofibers that undergo reversible switching between carbohydrate-hidden and exposed states on their surface in response to a thermal signal. Notably, this switching of the carbohydrate nanofibers leads to reversible capture and release of bacterial cells through controlled multivalent interactions, which subsequently regulates cell proliferation. We envisage that the incorporation of selective ligands at the surface of self-assembled nanostructures could generate switchable nanofibers to control many sophisticated biological functions such as signal transduction and protein inhibition.

Acknowledgements

This work was supported by the 1000 Program, NSFC (Grant 51473062 and 21450110416).

Notes and references

1 A. Imberty and A. Varrot, *Curr. Opin. Struct. Biol.*, 2008, **18**, 567.
2 C. R. Bertozzi and L. L. Kiessling, *Science*, 2001, **291**, 2357.
3 V. Wittmann and R. Pieters, *Chem. Soc. Rev.*, 2013, **42**, 4492.
4 P. Compain, C. Decroocq, J. Iehl, M. Holler, D. Hazelard, T. Mena Barragán, C. Ortiz Mellet and J.-F. Nierengarten, *Angew. Chem., Int. Ed.*, 2010, **49**, 5753.
5 M. Gingras, Y. M. Chabre, M. Roy and R. Roy, *Chem. Soc. Rev.*, 2013, **42**, 4823.
6 (*a*) J. E. Gestwicki, C. W. Cairo, L. E. Strong, K. A. Oetjen and L. L. Kiessling, *J. Am. Chem. Soc.*, 2002, **124**, 14922; (*b*) P. Wu, X. Chen, N. Hu, U. C. Tam, O. Blixt, A. Zettl and C. R. Bertozzi, *Angew. Chem., Int. Ed.*, 2008, **47**, 5022; (*c*) Y. M. Chabre and R. Roy, *Chem. Soc. Rev.*, 2013, **42**, 4657; (*d*) Y. Brissonnet, C. Ortiz Mellet, S. Morandat, M. I. Garcia Moreno, D. Deniaud, S. E. Matthews, S. Vidal, S. Šesták, E. K. Kirat and S. G. Gouin, *J. Am. Chem. Soc.*, 2013, **135**, 18427; (*e*) Y. M. Chabre, D. Giguère and B. Blanchard, *Chem. – Eur. J.*, 2011, **17**, 6545; (*f*) L. L. Kiessling, J. E. Gestwicki and L. E. Strong, *Angew. Chem., Int. Ed.*, 2006, **45**, 2348; (*g*) Y. Brissonnet, C. O. Mellet, S. Morandat, M. Isabel Garcia Moreno, D. Deniaud, S. E. Matthews, S. Vidal, S. Šesták, K. E. Kirat and S. G. Gouin, *J. Am. Chem. Soc.*, 2013, **135**, 18427.
7 (*a*) I.-B. Kim, J. N. Wilson and U. H. F. Bunz, *Chem. Commun.*, 2005, 1273; (*b*) K.-S. Krannig and H. Schlaad, *J. Am. Chem. Soc.*, 2012, **134**, 18542; (*c*) G. Pasparakis, A. Cockayne and C. Alexander, *J. Am. Chem. Soc.*, 2007, **129**, 11014.
8 (*a*) Y. Lim, K.-S. Moon and M. Lee, *Chem. Soc. Rev.*, 2009, **38**, 925; (*b*) G. B. Thomas, L. H. Rader, J. Park, L. Abezgauz, D. Danino, P. DeShong and D. S. English, *J. Am. Chem. Soc.*, 2009, **131**, 5471; (*c*) V. Percec, P. Leowanawat, H.-J. Sun, O. Kulikov, C. D. Nusbaum, T. M. Tran, A. Bertin, D. A. Wilson, M. Peterca, S. Zhang, M. P. Kamat, K. Vargo, D. Moock, E. D. Johnston, D. A. Hammer, D. J. Pochan, Y. Chen, Y. M. Chabre, T. C. Shiao, M. Bergeron-Brlek, S. André, R. Roy, H.-J. Gabius and P. A. Heiney, *J. Am. Chem.*

Soc., 2013, **135**, 9055; (*d*) A. Samanta, M. C. A. Stuart and B. J. Ravoo, *J. Am. Chem. Soc.*, 2012, **134**, 19909; (*e*) J. Brinkmann, E. Cavatorta, S. Sankaran, B. Schmidt, J. van Weerd and P. Jonkheijm, *Chem. Soc. Rev.*, 2014, **43**, 4449.

9 K. Petkau, A. Kaeser, I. Fischer, L. Brunsveld and A. P. H. J. Schenning, *J. Am. Chem. Soc.*, 2011, **133**, 17063.

10 D. A. Uhlenheuer, T. Petkau and L. Brunsveld, *Chem. Soc. Rev.*, 2010, **39**, 2817.

11 Y.-B. Lim, S. Park, E. Lee, J. H. Ryu, Y. R. Yoon, T. H. Kim and M. Lee, *Chem. – Asian J.*, 2007, **2**, 1363.

12 Y.-B. Lim, S. Park, E. Lee, H. Jeong, J.-H. Ryu, M. S. Lee and M. Lee, *Biomacromolecules*, 2007, **8**, 1404.

13 (*a*) M. K. Mueller and L. Brusveld, *Angew. Chem., Int. Ed.*, 2009, **48**, 2921; (*b*) K.-R. Wang, H.-W. An, Y.-Q. Wang, J.-C. Zhang and X.-L. Li, *Org. Biomol. Chem.*, 2013, **11**, 1007.

14 B. S. Kim, D. J. Hong, J. Bae and M. Lee, *J. Am. Chem. Soc.*, 2005, **127**, 16333.

15 J. H. Ryu, E. Lee, Y. Lee, Y. Lim and M. Lee, *J. Am. Chem. Soc.*, 2007, **129**, 4808.

16 D. W. Lee, T. Kim, I.-S. Park, Z. Huang and M. Lee, *J. Am. Chem. Soc.*, 2012, **134**, 14722.

17 (*a*) Y.-T. Chan, C. N. Moorefield and G. R. Newkome, *Chem. Commun.*, 2009, 6928; (*b*) K.-R. Wang, H.-W. An, Y.-Q. Wang, J.-C. Zhang and X.-L. Li, *Org. Biomol. Chem.*, 2013, **11**, 1007.

18 J. F. Lutz, K. Weichenhan, Ö. Akdemir and A. Hoth, *Macromolecules*, 2007, **40**, 2503.

19 (*a*) T. Kim, H. Lee, Y. Kim, J.-M. Nam and M. Lee, *Chem. Commun.*, 2013, **49**, 3949; (*b*) Z. Haung, H. Lee, S.-K. Kang, J.-M. Nam and M. Lee, *Nat. Commun.*, 2011, **2**, 459; (*c*) H.-J. Kim, S.-K. Kang, Y.-K. Lee, C. Seok, J.-K. Lee, W.-C. Zin and M. Lee, *Angew. Chem., Int. Ed.*, 2010, **122**, 8649; (*d*) Z. Huang, S.-K. Kang, M. Banno, T. Yamaguchi, D. Lee, C. Seok, E. Yashima and M. Lee, *Science*, 2012, **337**, 1521.

20 C. W. Cairo, J. E. Gestwicki, M. Kanai and L. L. Kiessling, *J. Am. Chem. Soc.*, 2002, **124**, 1615.

21 H. Wang, L. Gu, Y. Lin, F. Lu, M. J. Meziani, P. G. Luo, W. Wang, L. Cao and Y. P. Sun, *J. Am. Chem. Soc.*, 2006, **128**, 13364.

22 P. G. Luo, H. Wang, L. Gu, F. Lu, Y. Lin, K. A. Christensen, S. T. Yang and Y. P. Sun, *ACS Nano*, 2009, **3**, 3909.

23 B. Wang, P. Liu, W. Jiang, H. Pan, X. Xu and R. Tang, *Angew. Chem., Int. Ed.*, 2008, **47**, 3560.

24 J. Kim, Y. Ahn, K. M. Park, D.-W. Lee and K. Kim, *Chem. – Eur. J.*, 2010, **16**, 12168.

25 Y. Kim, J. Kang, B. Shen, Y. Wang, Y. He and M. Lee, *Nat. Commun.*, 2015, **6**, 8650.

26 M. D. Disney, J. Zheng, T. M. Swager and P. H. Seeberger, *J. Am. Chem. Soc.*, 2004, **126**, 13343.

27 H.-J. Kim, E. Lee, H.-S. Park and M. Lee, *J. Am. Chem. Soc.*, 2007, **129**, 10994.

28 J. H. Prestegard, V. W. Miner and P. M. Tyrell, *Proc. Natl. Acad. Sci. U. S. A.*, 1983, **80**, 7192.

